National Cooperative Highway Research Program

RESEARCH RESULTS DIGEST

DIGEST 60 - APRIL 1974

LIBRARY
MAY 30 1974
TRANSPORTATION RESEARCH BOARD

These **Digests** are issued in the interest of providing an early awareness of the research results emanating from projects in the NCHRP. By making these results known as they are developed and prior to publication of the project report in the regular NCHRP series, it is hoped that the potential users of the research findings will be encouraged toward their early implementation in operating practices. Persons wanting to pursue the project subject matter in greater depth may obtain, on a loan basis, an uncorrected draft copy of the agency's report by request to the NCHRP Program Director, Highway Research Board, 2101 Constitution Ave., N.W., Washington, D.C. 20418

Fatigue of Welded Steel Bridge Members Under Variable-Amplitude Loadings

An NCHRP staff digest of the essential findings from progress reports on NCHRP Project 12-12, "Welded Steel Bridge Members Under Variable-Cycle Fatigue Loadings," by C. G. Schilling, K. H. Klippstein, J. M. Barsom, and G. T. Blake, Research Laboratory, United States Steel Corporation, Monroeville, Pa.

THE PROBLEM AND ITS SOLUTION

The American Association of State Highway and Transportation Officials (AASHTO) has recently adopted new fatigue design provisions based on constant-amplitude fatigue data obtained in NCHRP Project 12-7, "Effect of Weldments on Fatigue Strength of Steel Beams," conducted at Lehigh University. According to these new provisions, which are considerably simpler than the previous AASHTO fatigue provisions, bridges are designed so that they can withstand a certain number of constant-amplitude cycles of stress equal to the design live-load plus impact stress. The required constant-stress cycles were developed using Miner's law for cumulative damage to reflect the estimated volume of truck traffic causing variable-amplitude stress cycles that are usually well below the design live-load stresses. The new provisions are expected to result in conservative designs.

There are still gaps in the available information. Specifically, information is needed on (1) the magnitude and frequency of traffic loadings on bridges, (2) the actual stress caused by these traffic loadings, and (3) the fatigue life of various types of bridge members under variable-amplitude loadings. Consequently, NCHRP and others have initiated studies to obtain this information.

NCHRP Project 12-12, "Welded Steel Bridge Members Under Variable-Cycle Fatigue Loadings," deals with the third part of the problem. Its objectives are to acquire fatigue data on welded bridge members under variable-amplitude random-sequence stress spectrums, such as occur in actual bridges, and to develop an analytical method of predicting variable-amplitude fatigue behavior from constant-amplitude fatigue data. To accomplish these objectives, the following tasks are being performed:

1. A study of pertinent past work, with particular emphasis on field measurements of stresses in bridges under traffic.
2. A theoretical study to predict from various hypotheses the fatigue behavior of the small specimens and beams being tested during the program.

HIGHWAY RESEARCH BOARD
NATIONAL RESEARCH COUNCIL
NATIONAL ACADEMY OF SCIENCES—NATIONAL ACADEMY OF ENGINEERING

3. A program of variable- and constant-amplitude fatigue tests of small specimens to obtain crack growth data and to determine the effects of various stress-spectrum parameters on fatigue life.
4. A program of variable- and constant-amplitude fatigue tests of relatively large beams of various steels, with bridge details similar to those tested in NCHRP Project 12-7 *(NCHRP Report 102)*.
5. An evaluation of the results and development of methods of utilizing the results for design and specification purposes.

Initially, the research agency concentrated on collection and evaluation of field stress measurements of bridges under traffic. These data were obtained from the Federal Highway Administration and various state highway departments. After completing the review of field data, the agency selected distributions for the variable-amplitude stress spectra to be used in the experimentation. In addition, considerable effort went into planning an experimental program on small plate specimens and large beam specimens.

The experimental program consists of:

1. Some 80 cover-plate specimens of ASTM A514 steel (Fig. 1), used to study the effects of stress-spectrum parameters. Use of a large number of relatively small plate specimens permitted study of secondary variables that could not be included in the beam testing program.
2. Wedge-opening-loading (WOL) specimens (Fig. 2), used to obtain basic crack growth data for A514 steel. Numerous crack extension measurements were made during each test.
3. Some 156 cover-plated beams (Fig. 3), used to obtain the approximate lower bound for the variable-amplitude fatigue strength of fabricated bridge members. Of these, 48 were fabricated from A36 steel and the rest from A514 steel.
4. Some 66 welded beams (Fig. 4) used to obtain the approximate upper bound for fabricated bridge members. Of these, 36 were fabricated from A36 steel and the rest from A514 steel.

NCHRP Project 12-12 began at U. S. Steel's Research Laboratory in October 1970. Items 1, 2, and 3 have been completed; item 4 was started in late 1973 and is now in progress. This Research Results Digest is based in part on the agency's October 1972 interim report. Section I of that report describes the material properties and fabrication methods for the beams and specimens. Section II describes the test setup and procedures for the plate-specimen and the beam tests. Section III summarizes available field measurements of stresses under traffic in short-span bridges and describes the stress spectra that were developed from these measurements for use in the testing program. Section IV describes the fatigue crack growth behavior of A514 steel under the variable-amplitude random-sequence stress spectra developed in Section III. The October 1972 interim report will not be published, but loan copies are available on request to the NCHRP Program Director. A final report on this project is expected to be available by mid-1975. The purpose of this Research Results Digest is the early dissemination of some results and tentative findings from this research. These tentative findings could be immediately useful to bridge engineers in assessing the life expectancy of critical structures. The final results from this study will be useful in evaluating the AASHTO design specifications as they relate to variable-amplitude fatigue and could eventually lead to fatigue design methods based on more realistic loadings.

FINDINGS

The review of field data showed that passage of a vehicle over a bridge produces a single major stress cycle, with superimposed vibrational stress cycles, as illustrated by the typical stress traces in Figure 5a. For most types of short-span bridges the vibrational stress cycles are small enough to be neglected.* The major stress cycle adds to the deadload stress, as idealized in Figure 5b. Therefore, as shown in Figure 6a, the stress spectrum, or stress history, for a particular point in a bridge can be defined in terms of the frequency of occurrence of stress ranges, S_r, of different magnitudes and the minimum (dead load) stress, S_{min}, which remains essentially constant during the life of the bridge. Stress range ($S_{max} - S_{min}$) is used to define the major stress cycles in this study, because it has been found to be the most important stress parameter affecting the fatigue strength of bridge members.

*For cantilever (suspended-span) girder bridges, the passage of a vehicle often produces many large stress cycles as a result of the vibrational characteristic of such bridges.

In Figure 6a, the frequency of occurrence of stress ranges is defined by a histogram, or bar graph, in which the height of the bar represents the percentage of stress ranges within an interval represented by the width of the bar. The frequency-of-occurrence data can be presented in a more general way by dividing the height of each bar by the width of the bar to obtain a probability-density curve such as shown in Figure 6b. The area under this curve between any two values of S_r represents the percentage of occurrences within that interval.

A single nondimensional mathematical expression can be used to define the probability-density curves for different sets of data. The study of field data showed that the following nondimensional mathematical expression, which defines a family of skewed probability-density curves referred to as Rayleigh curves,* can be used to accurately fit a probability-density curve to each available set of field data:

$$p' = 1.011x'e^{-1/2(x')^2} \qquad (1)$$

in which $x' = (S_r - S_{rmin})/S_{rd}$ and S_{rmin} is the minimum stress range in the spectrum. Eq. 1 is plotted at the top of Figure 7. As illustrated at the middle of Figure 7, a particular curve from the family is defined by two parameters: (1) the modal stress range, S_{rm}, which corresponds to the peak of the curve; and (a) the parameter S_{rd}, which is a measure of the width of the curve, or the dispersion of the data. The curve could be shifted sideways by changing S_{rm} and the width of the curve could be modified by changing S_{rd}. Mathematical expressions for the modal, median, mean, and root-mean-square values of the spectrum are given in Figure 7. The root-mean-square (RMS) value is defined as the square root of the mean of the squares of the individual values of x' or S_r.

The probability-density curves being used in the testing program are defined by S_{rm} and S_{rd}/S_{rm}; a set of curves for a single value of S_{rm} and for the four values of S_{rd}/S_{rm} being used in the testing program is shown at the bottom of Figure 7. $S_{rd}/S_{rm} = 0$ corresponds to constant-amplitude loading in which all cycles are at S_{rm}. The control tapes used in the fatigue testing program contain 500 individual stress ranges that satisfy one of these Rayleigh probability-density curves and are arranged in a random sequence. The tape is continuously cycled throughout a test while S_{min} is held constant. A typical portion of the 500-cycle, variable-amplitude ($S_{rd}/S_{rm} = 1.0$), random-sequence loading block in shown in Figure 8.

Test Results. Results of most of the completed fatigue tests are given in Table 1. Except as indicated in the footnotes, the number of cycles listed is a log-average** fatigue life to failure for three replicate specimens. The table is self-explanatory with the exception of reference to details A, B, and C in the case of the cover-plated beams. It was determined during the study that fabrication techniques have a significant influence on fatigue life. Beams with cover plates welded to the flanges before the flanges were welded to the web (detail A) endured considerably more cycles of stress before failure than did those with flange-to-web welds made before attachment of the cover plates (detail B). It is theorized that in the former case the flange-to-web welds relieve the tensile residual stresses that result from the cover-plate weld. Although this has a beneficial effect on fatigue life, it is not likely to be useful in practice, where cover plates are not usually welded to plate girders. To ensure that the detail tested would provide a realistic lower limit on the fatigue strength of fabricated bridge girders and would be comparable with the cover-plate end detail tested in NCHRP Project 12-7, all remaining cover-plated beams (detail A) were cross welded to produce detail C.

For brevity, only the results for detail C are discussed in detail herein; the results for the other types of specimens follow the same trends and will be discussed in the final report. In Figure 9, the modal stress range is plotted against the life for detail C. Inasmuch as previous work and the present study show that steel strength and minimum stress are secondary parameters in fatigue behavior, the data for A36 and A514 steels and for S_{min} equal to 0 and 10 ksi are plotted on a single graph. Furthermore, to avoid cluttering the graph with too many overlapping data points, a single point is plotted for each combination of S_{rm} and S_{rd}/S_{rm}. This point represents the log-average for all the individual tests, usually six or more, at that combination of S_{rm} and S_{rd}/S_{rm}. Points are plotted only at two values of S_{rm} and three values of S_{rd}/S_{rm}, where considerable data are available; isolated data at other values of S_{rm} or S_{rd}/S_{rm} are not plotted.

*The full Rayleigh curve extends to infinity, but the curve defined by Equation 1 is truncated at $x' = 3$. Because the area under the full curve beyond $x' = 3$ is 1.1 percent of the total area, the constant 1.011 has been inserted into the mathematical expression to make the area under the truncated curve equal 1.000.

**The log-average, which is the anti-log of the mean of the logs of a set of lives, is used because log N is a linear function of log S_r discussed later; therefore, the log-average of a set of data points has the same effect in curve fitting as the individual points in the set.

Past and present studies suggest that fatigue data can be approximated by a straight line on a log-log plot; this line is defined by

$$\log N = A - B \log S_{rm} \tag{2}$$

in which A and B are constants selected to provide a best-fit line for available data. A best-fit line defined by Eq. 2 is plotted for each different value of S_{rd}/S_{rm}. These lines are roughly parallel and show that the life corresponding to a given S_{rm} decreases as S_{rd}/S_{rm}, which is a measure of the spectrum width, increases, although the scatter bands for different values of S_{rd}/S_{rm} overlap.

Effective Stress Range. There are many ways of relating variable-amplitude fatigue data to constant-amplitude data; probably the most convenient for bridge applications is the effective stress-range concept, which will permit the three lines in Figure 9 to be approximated by a single line relating the effective-stress range, S_{re}, to the life, N. The effective stress range for a variable-amplitude spectrum is defined as the constant-amplitude stress range that would result in the same fatigue life as the variable-amplitude spectrum. Several different methods of calculating S_{re} are being evaluated in the present study. Two that give reasonable results are discussed in the following.

In the first of these, which is based directly on the Rayleigh distribution discussed earlier, the effective stress range is given by

$$S_{re} = S_{rm} + C\, S_{rd} \tag{3}$$

in which the best-fit value of the correlation factor, C, is determined from available data. If $C = 0.378$, S_{re} is the root-mean-square of all stress ranges in the spectrum; if $C = 0.230$, S_{re} is the mean of the stress ranges (see Fig. 7). The variation of S_{re}/S_{rm} with S_{rd}/S_{rm} for these two values of C is shown in Figure 10.

Values of C determined experimentally for various test cases (including specimens other than detail C) are given in Table 2. Although C varies significantly for various cases, the root-mean-square value of 0.378 provides a reasonable approximation of C for practical purposes. The difference between this approximate value of C and the true value for a particular case has only a small effect on S_{re}. All data for detail C are plotted in Figure 11 in terms of $S_{re_{RMS}}$. Also shown are the solid line representing the best fit of the constant-amplitude data and two dashed lines two standard errors of estimate from the solid. The figure shows that $S_{re_{RMS}}$ provides a satisfactory method of relating variable-amplitude data to constant-amplitude data.

The root-mean-square stress range can be calcualted either by fitting a Rayleigh curve to the spectrum or directly from

$$S_{re_{RMS}} = \left(\sum \alpha_i S_{ri}^2\right)^{1/2} \tag{4}$$

where S_{ri} is the ith stress range in the spectrum and α_i is the fraction of stress ranges of that magnitude.

The second method of calculating the effective stress range is based on the widely used Miner's Law, which states that

$$\sum \frac{\alpha_i N}{N_i} = 1.0 \tag{5}$$

in which N is the fatigue life for a variable-amplitude spectrum, N_i is the fatigue life for a constant-amplitude loading corresponding to the ith stress range in the spectrum, and α_i is the fraction of stress ranges of that magnitude. By definition, the life, N, for the variable-amplitude spectrum is the same as the life, N , for a constant-amplitude loading of S_{re} and is given by Eq. 2, which can be expressed in the form

$$N = \frac{10^A}{S_{re}^B} \tag{6}$$

The value of N_i is given by a similar equation in which S_{re} is replaced by S_{ri}. Hence,

$$\sum \alpha_i \left(\frac{10^A}{S_{re}^B}\right)\left(\frac{S_{ri}^B}{10^A}\right) = 1.0 \qquad (7)$$

and

$$S_{re} = \left(\sum \alpha_i S_{ri}^B\right)^{1/B} \qquad (8)$$

B is the slope of the log-log S - N curve (= about 3 for most details).

Thus, Eq. 8 is similar to Eq. 4 but the S_{ri} term is cubed rather than squared. The variation of S_{re}/S_{rm} with S_{rd}/S_{rm} for a spectrum defined by a Rayleigh curve and for B = 3 is plotted in Figure 10.

All data for detail C are plotted in Fig. 12 in terms of $S_{re_{MINER}}$. The residual sum of the squares, RSS, shown on the figure is a measure of the closeness of fit of the variable-amplitude data to the best-fit line for the constant-amplitude data; the smaller the RSS the better the fit. For $S_{re_{MINER}}$ the RSS is 1.69 compared with 1.25 for $S_{re_{RMS}}$. Thus, $S_{re_{RMS}}$ provides a better fit of the plotted data than $S_{re_{MINER}}$; similarly, $S_{re_{RMS}}$ provided a somewhat better fit than $S_{re_{MINER}}$ for most of the combinations of detail and steel considered in the test program. Nevertheless, $S_{re_{MINER}}$ does not provide a reasonable approximation for all combinations.

Comparison With AASHTO Design Provisions. In Figure 13, all cover-plated beam data from the present study are compared with recently adopted AASHTO fatigue design provisions. Specifically, the present results are compared with the specified fatigue strength for cover-plate ends (AASHTO Category E) on the basis of $S_{re_{RMS}}$. The specified fatigue strength line closely approximates the lower limits (95% confidence limit) of previous constant-amplitude test results on cover-plate-ends details. All except two data points are above the line; these two fall only slightly below the line. This shows that the AASHTO fatigue strength line provides an approximate lower limit for variable-amplitude test results that are plotted on the basis of the root-mean-square effective stress range, and that the results of the present study are consistent with previous experimental results. The scatter in the Figure 13 results is reasonable considering that data for different steels, minimum stress details, and welding sequences are included in a single plot.

APPLICATIONS

The results of this study provide a link between the type of variable-amplitude random-sequence fatigue loadings that actually occur on bridges and the constant-amplitude fatigue data and allowable-stress values that are commonly used in designing such bridges. Consequently, the results should be useful to design engineers, specification writers, and researchers, and could eventually lead to AASHTO fatigue design methods based on more realistic loadings. Furthermore, the results can be used by bridge designers to calculate (1) the remaining life of existing bridges, especially old bridges that were originally designed for lighter loads or contain undesirable design details, and (2) the design life of new bridges that are frequently subjected to unusual loading conditions.

Four steps are required in estimating the remaining life of a bridge: (1) develop a histogram (frequency-of-occurrence bar graph) for the stress spectrum at each critical detail and an estimate of the number of cycles per day, (2) calculate the effective (constant-amplitude) stress range for the spectrum, (3) develop a curve or equation of the allowable constant-amplitude stress range vs number of cycles for each critical detail, and (4) calculate the fatigue life for each detail. These steps are discussed in the following and illustrated by an example problem. In this example, (summarized in Figure 14) the remaining life for an end detail of the hangers on a 10-year-old truss bridge is calculated. This example was selected to illustrate severe fatigue conditions not representative of the conditions in most highway bridges.

The cyclic stress range, which usually corresponds to the passage of a single truck, is the main parameter in the fatigue analysis. (Stress cycles caused by cars can be neglected.) Consequently, the type of histogram shown in Figure 14 is used; the height of each bar represents the percentage of stress ranges within an interval defined by the width of the bar. The most reliable method of obtaining such a histogram for an existing bridge is to make field measurements of the

nominal stresses* at critical details while the bridge is under normal traffic. Although this method is expensive, it may be justified in a few critical cases. A second way to obtain the needed stress-range histogram is to estimate it from measured or predicted data on truck traffic at the location of the bridge. Field measurements have shown that the actual stresses in bridges due to live loads plus impact are almost always well below the corresponding design stresses because of various conservative factors in the design procedures. Consequently, realistic parameters based on past experience or available field measurements on similar bridges must be used to estimate the stress ranges corresponding to given trucks. An empirical method of doing this for certain types of bridges is given in the paper, "Loading History Analysis of Steel Weldments in Bridge Structures," by Heins and Galambos.** A third way to obtain the needed histogram is to estimate it directly from field data on similar bridges.

To predict the remaining or total life of a bridge in years, it it necessary to estimate the past and future traffic volumes for the bridge. Specifically, it is necessary to know the total number of daily occurrences of the stress ranges defined in the histogram. Passage of a truck usually causes a single major stress cycle; but in certain types of bridges, such as suspended-span girder bridges, such a passage has been found to cause a large number of stress cycles as a result of bridge vibrations. Consequently, the type of bridge must be considered when estimating the number of daily stress cycles from the expected traffic volume. In the example, the number of daily stress cycles is taken to be 1,000.

The effective (constant-amplitude) stress range for the stress spectrum defined by a histogram can be taken as the root-mean-square of the stress ranges in the histogram and can be calculated from Eq. 4. The effective stress range for the example spectrum was calculated to be 4.38 ksi, as shown in Figure 14.

A curve or equation for the allowable constant-amplitude stress range for a particular detail can be obtained from the recently adopted AASHTO fatigue provisions or from available test data, such as are given in *NCHRP Report 102*, "Effect of Weldments on the Fatigue Strength of Steel Beams." To obtain a curve from the AASHTO provisions for category E, the allowable stress ranges for three life categories (100,000, 500,000 and 2,000,000 cycles) are plotted and a straight line is drawn through these points, as shown in Figure 14. Similarly, an equation for this curve could be obtained as shown in the figure. Such AASHTO curves and equations approximate the lower limits (95 percent confidence limit) of test results.

The fatigue life for a particular detail can be determined from the AASHTO constant-amplitude (effective stress range) curve or equation for that detail; the value of N corresponding to the effective stress range for the spectrum (4.38 ksi) gives a reasonable estimate of the total number of cycles to failure (13.0×10^6). (The percentage of these cycles that fall within any particular interval of stress ranges is given by the histogram.) The expected life in years can be calculated by dividing the total number of cycles (13.0×10^6) by the estimated number of cycles per year ($365 \times 1{,}000$). Thus, in the example, the expected total life for the critical detail is 35.6 years and the remaining life is 25.6 years.

---

*Because the available fatigue curves for various details are based on nominal stresses, the measured stresses that are related to these curves should also be based on nominal stresses. Consequently, the stresses should be measured far enough from a critical detail to eliminate local stress concentrations.

**Presented at 53rd Ann. Meeting, Highway Research Board, to be published in a Highway Research Record during 1974.

Table 1

Fatigue Test Results

Set No.	S_{min} (ksi)	S_{rm} (ksi)	S_{rd}/S_{rm}	No. of Cycles [a] (Mil.)	Steel Type	Test Article [g]
1	0	10	0.0	15.3 [b]	A514	Cover-plated beam detail A
2	0	10	0.5	— [c]	A514	Cover-plated beam detail A
3	0	10	1.0	2.11	A514	Cover-plated beam detail A
4	0	20	0.0	0.90	A514	Cover-plated beam detail A
5	0	20	0.5	0.49	A514	Cover-plated beam detail A
6	0	20	1.0	0.20	A514	Cover-plated beam detail A
7	0	30	0.0	0.12	A514	Cover-plated beam detail A
8	0	30	0.5	0.17	A514	Cover-plated beam detail A
10	10	10	0.0	2.55	A514	Cover-plated beam detail A
11	10	10	0.5	1.77	A514	Cover-plated beam detail A
12	10	10	1.0	0.84	A514	Cover-plated beam detail A
13	10	20	0.0	0.48	A514	Cover-plated beam detail A
14	10	20	0.5	0.27	A514	Cover-plated beam detail A
15	10	20	1.0	0.21	A514	Cover-plated beam detail A
16	10	30	0.0	0.10	A514	Cover-plated beam detail A
17	10	30	0.5	0.10	A514	Cover-plated beam detail A
19	10	60	0.0	0.01	A514	Cover-plated beam detail A
20	10	4	1.0	8.44 [d]	A514	Cover-plated beam detail A
22	40	10	0.0	1.48	A514	Cover-plated beam detail A
23	40	10	0.5	1.04	A514	Cover-plated beam detail A
24	40	30	0.0	0.06	A514	Cover-plated beam detail A
25	40	30	0.5	0.05	A514	Cover-plated beam detail A
26	0	10	0.0	1.86	A514	Cover-plated beam detail B
27	0	10	1.0	0.93	A514	Cover-plated beam detail B
28	10	10	0.0	1.27	A514	Cover-plated beam detail C
29	10	10	0.5	1.17	A514	Cover-plated beam detail C
30	10	10	1.0	0.47	A514	Cover-plated beam detail C
31	10	20	0.0	0.23	A514	Cover-plated beam detail C
32	10	20	0.5	0.17	A514	Cover-plated beam detail C
33	10	20	1.0	0.10	A514	Cover-plated beam detail C
34	10	30	0.0	0.08	A514	Cover-plated beam detail C
35	10	30	0.5	0.07	A514	Cover-plated beam detail C
36	0	10	0.0	1.40	A514	Cover-plated beam detail C
37	0	10	1.0	0.73	A514	Cover-plated beam detail C
101	0	10	0.0	1.60	A36	Cover-plated beam detail C
102	0	10	0.25	0.83	A36	Cover-plated beam detail C
103	0	10	0.5	0.61	A36	Cover-plated beam detail C
104	0	20	0.0	0.15	A36	Cover-plated beam detail C
105	0	20	0.25	0.13	A36	Cover-plated beam detail C
106	0	20	0.5	0.10	A36	Cover-plated beam detail C
107	10	10	0.0	1.99	A36	Cover-plated beam detail A
108	10	10	0.25	1.78	A36	Cover-plated beam detail A
109	10	10	0.5	1.04	A36	Cover-plated beam detail A
110	10	20	0.5	0.21	A36	Cover-plated beam detail A
111	10	10	0.25	0.16	A36	Cover-plated beam detail A
113	0	40	0.0	0.02	A36	Cover-plated beam detail C
114	0	5	0.5	5.97	A36	Cover-plated beam detail C
115	0	10	0.0	1.61 [e]	A36	Cover-plated beam detail A
116	10	10	0.0	0.97	A36	Cover-plated beam detail C
117	10	10	0.5	0.53	A36	Cover-plated beam detail C
501	0	10	0.0	15.20 [f]	A514	Cover-plate specimen
502	0	10	0.5	3.95	A514	Cover-plate specimen
503	0	10	1.0	2.39	A514	cover-plate specimen
504	0	30	0.0	.24	A514	Cover-plate specimen
505	0	30	0.5	0.18	A514	Cover-plate specimen
506	0	30	1.0	0.14	A514	Cover-plate specimen
507	10	10	0.0	4.40	A514	Cover-plate specimen
508	10	10	0.5	3.56	A514	Cover-plate specimen
509	10	10	1.0	2.08	A514	Cover-plate specimen
510	10	30	0.0	0.24	A514	Cover-plate specimen
511	10	30	0.5	0.18	A514	Cover-plate specimen
512	10	30	1.0	0.12	A514	Cover-plate specimen
513	10	60	0.0	0.04	A514	Cover-plate specimen
514	10	4	1.0	——	A514	Cover-plate specimen
515	40	10	0.0	5.61	A514	Cover-plate specimen
516	40	10	0.5	2.46	A514	Cover-plate specimen
517	40	30	0.0	0.23	A514	Cover-plate specimen
518	40	30	0.5	0.14	A514	Cover-plate specimen

[a] Log-average (anti-log of the mean of the logs) for three replicate tests unless otherwise noted. [b] Plus two beams unfailed at 10 million. [c] All three beams unfailed at 11 million. [d] Plus two beams unfailed at 20 million. [e] Plus one beam unfailed at 6.6 million. [f] Plus one specimen unfailed at 25 million. [g] Detail A = cover-plate ends not cross welded, web-flange welds made last; detail B = cover-plate ends not cross welded, cover-plate welds made last; detail C = cover-plate ends cross welded.

TABLE 2

Correlation Factor

Detail [a]	Steel	S_{min} ksi	Correlation Factor, C [b] S_{rd}/S_{rm}=0.25	S_{rd}/S_{rm}=0.50	S_{rd}/S_{rm}=1.0	Combined [c]	Number of Tests [d]
Cover plate A	A514	0	--	0.070	0.453	0.378	18
Cover plate A	A514	10	--	0.271	0.356	0.360	21
Cover plate A	A514	0,10	--	0.228	0.414	0.355	27
Cover plate C	A514	10	--	0.140	0.419	0.364	24
Cover plate S	A514	0	--	0.217	0.250	0.275	15
Cover plate S	A514	10	--	0.180	0.296	0.285	21
Cover plate S	A514	0,10	--	0.177	0.270	0.270	36
Cover plate A	A36	10	0.211	0.434	---	0.395	15
Cover plate C	A36	0	0.508	0.470	---	0.452	24

[a] A = beams with cover-plate ends not cross welded and web-flange welds placed last; C = beams with cover-plate ends cross welded last; S = cover-plate specimens with cover-plate ends not cross-welded.

[b] Factor based on $\log N = A - B \log S_{re}$, with $S_{re} = S_{rm} + CS_{rd}$, and combined test data for $S_{rd}/S_{rm} = 0.0$ (constant amplitude) and the value of S_{rd}/S_{rm} shown.

[c] Includes data for all values of S_{rd}/S_{rm}.

[d] Number of tests included in combined data.

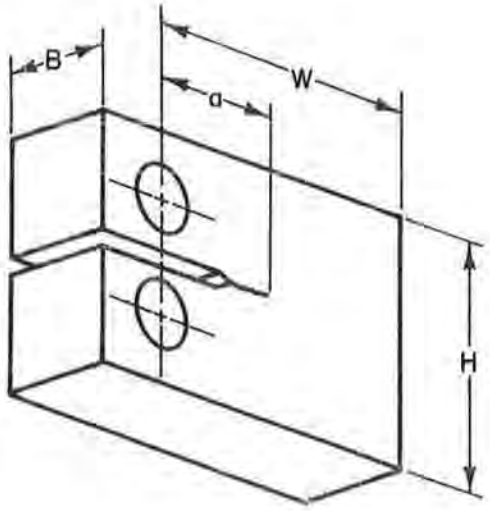

a -CRACK LENGTH
B -SPECIMEN THICKNESS
W -SPECIMEN WIDTH
H -SPECIMEN HEIGHT

NOMINAL DIMENSIONS
a = 1.0 inch (25.4 mm)
B = 0.37 inch (9.4 mm)
W = 2.55 inches (64.77 mm)
H = 2.48 inches (62.99 mm)

Figure 2. Geometry of wedge-opening-loading (WOL) specimen.

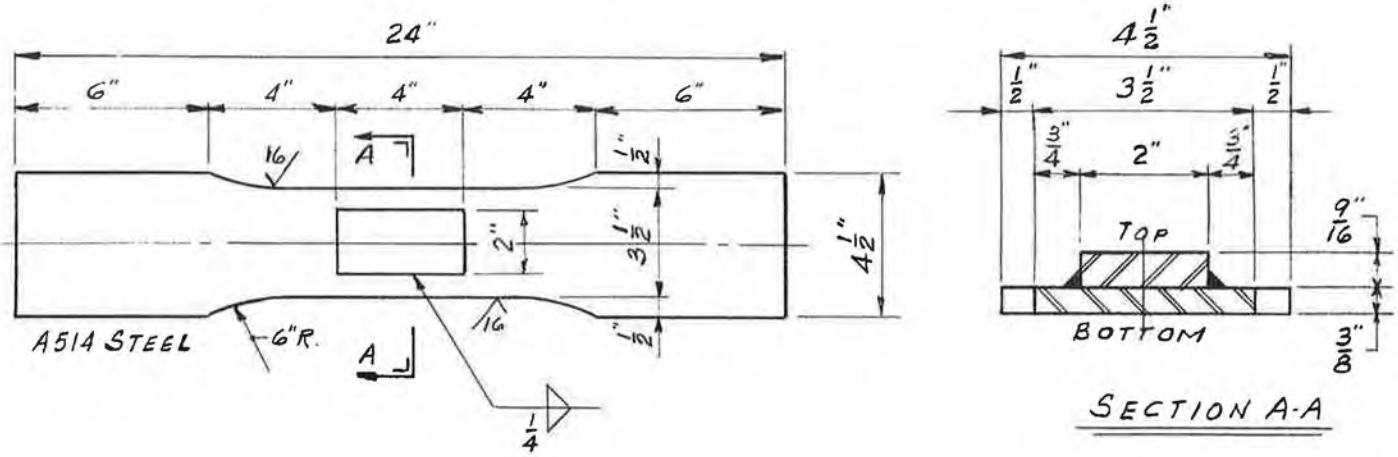

Nominal Section Modulus	Top:	0.337 $in.^3$	Bottom:	0.441 $in.^3$
Nominal Moment of Inertia		0.179 $in.^4$		
Mean Section Modulus	Top:	0.352 $in.^3$	Bottom:	0.461 $in.^3$
Mean Moment of Inertia		0.191 $in.^4$		

Figure 1. Cover-plate specimens.

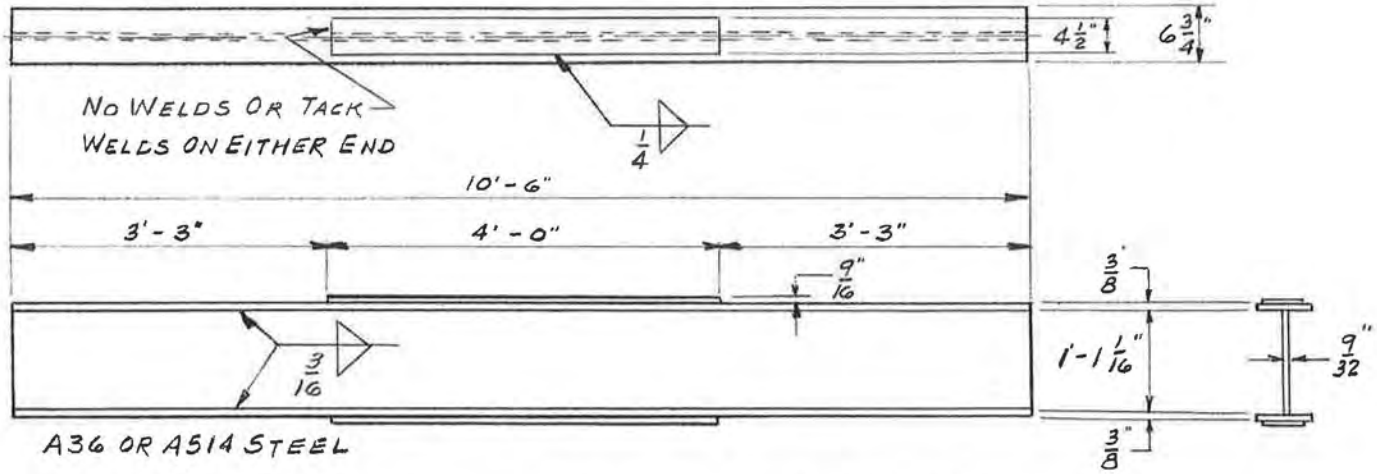

	A36	A514
Nominal Section Modulus	73.8 in.^{3}	
Nominal Moment of Inertia	552 in.^{4}	
Mean Section Modulus	74.3 in.^{3}	75.7 in.^{3}
Mean Moment of Inertia	556 in.^{4}	567 in.^{4}

Figure 3. Cover-plated beams.

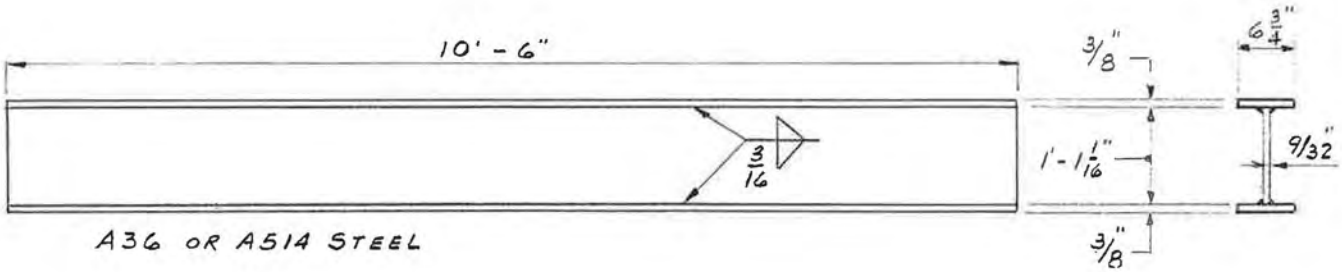

Nominal Section Modulus	41.1 in.^{3}	
Nominal Moment of Inertia	284 in.^{4}	
	A36	A514
Mean Section Modulus	41.3 in.^{3}	42.1 in.^{3}
Mean Moment of Inertia	286 in.^{4}	291 in.^{4}

Figure 4. Welded beams.

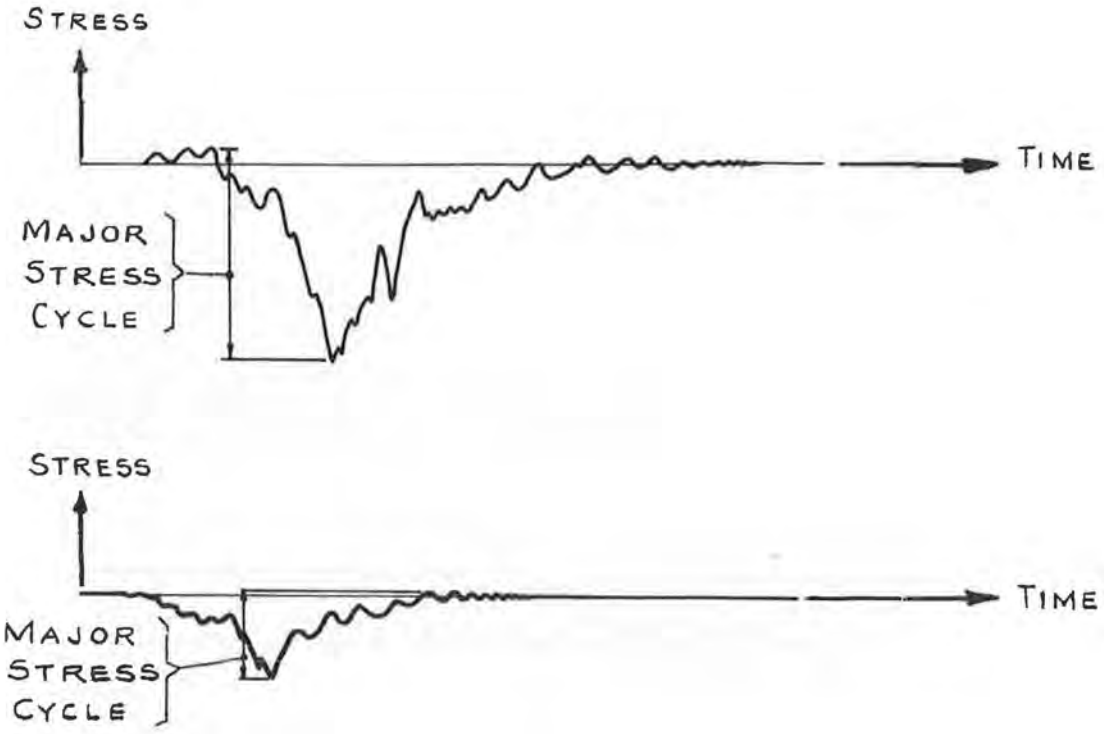

ACTUAL STRESS TRACES FIG. 5a

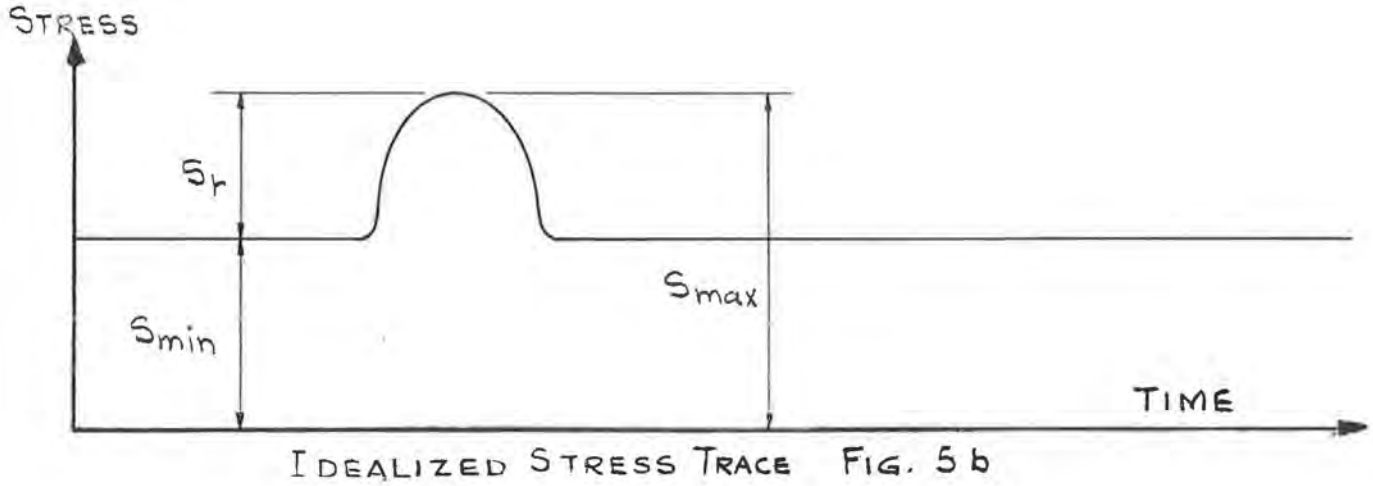

IDEALIZED STRESS TRACE FIG. 5b

Figure 5. Stress traces for passage of a single vehicle.

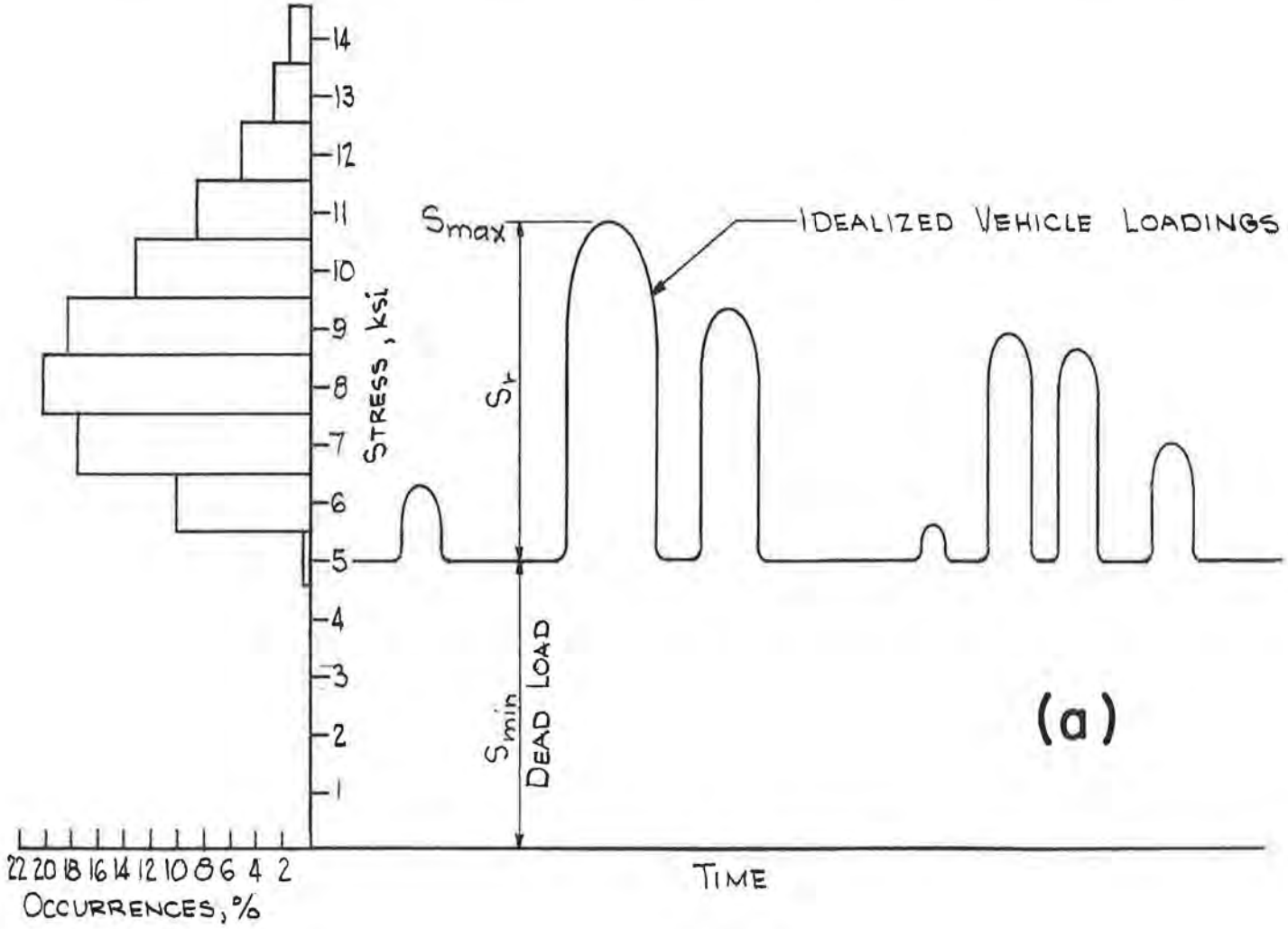

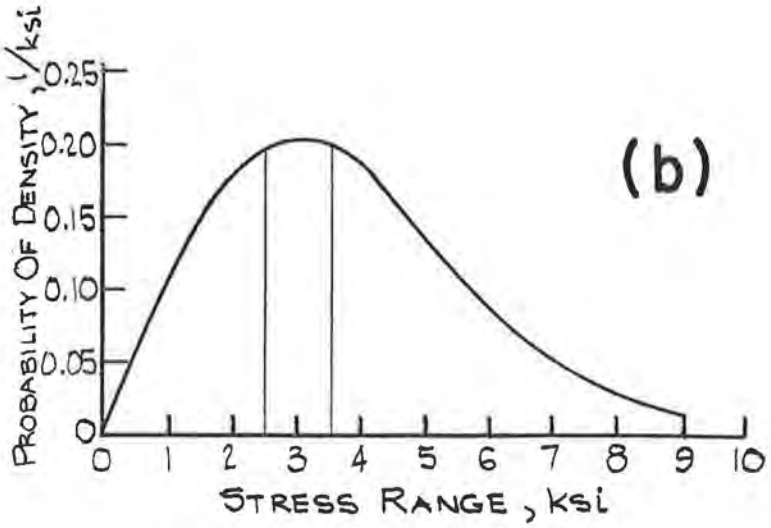

Figure 6. Frequency-of-occurrence data.

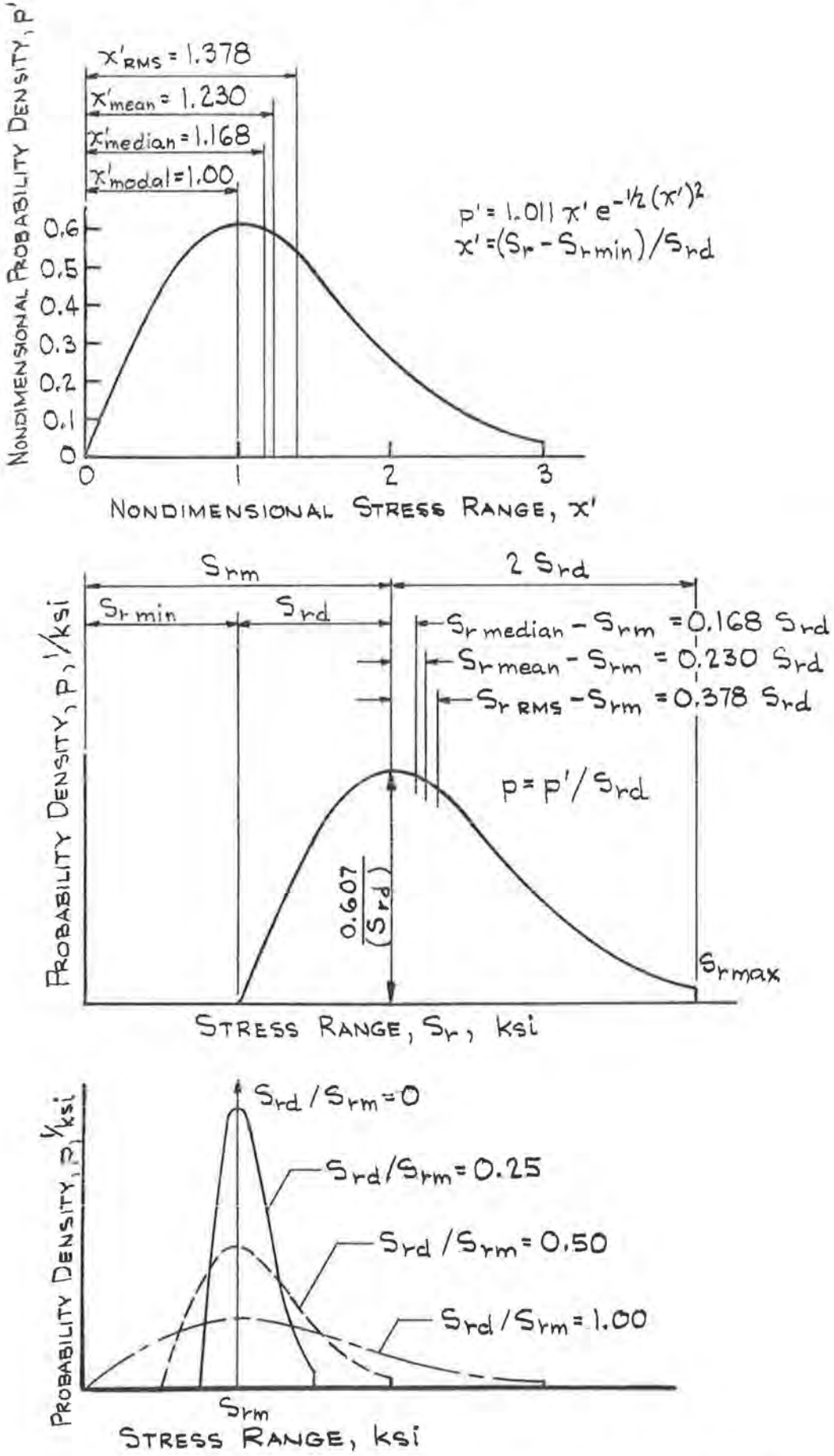

Figure 7. Characteristics of Rayleigh probability curves.

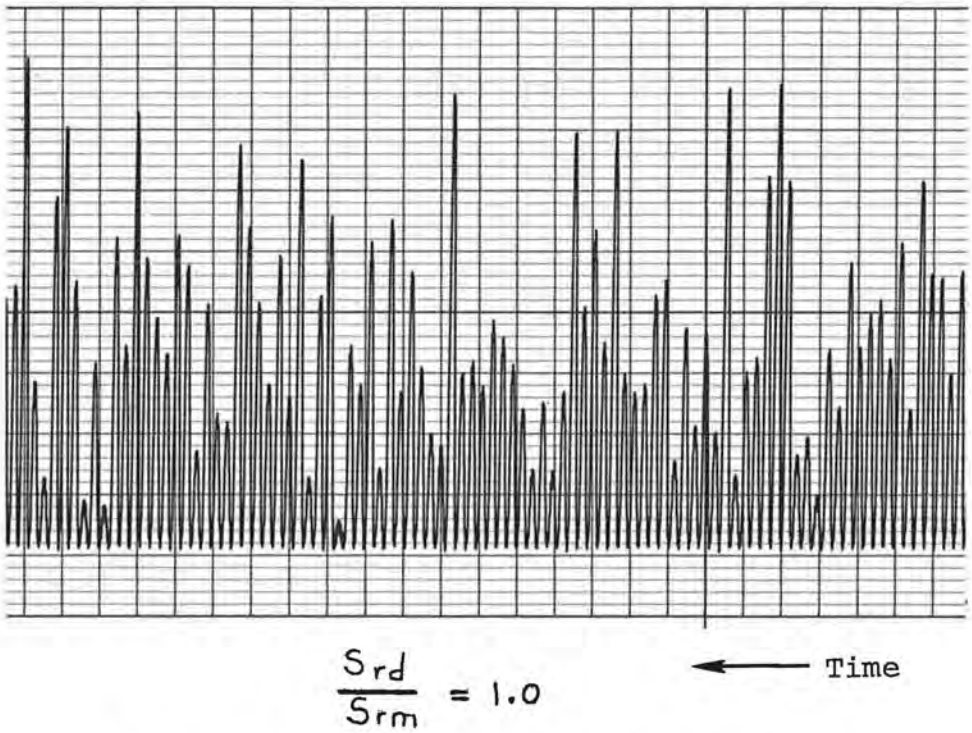

Figure 8. Portion of a typical strain record.

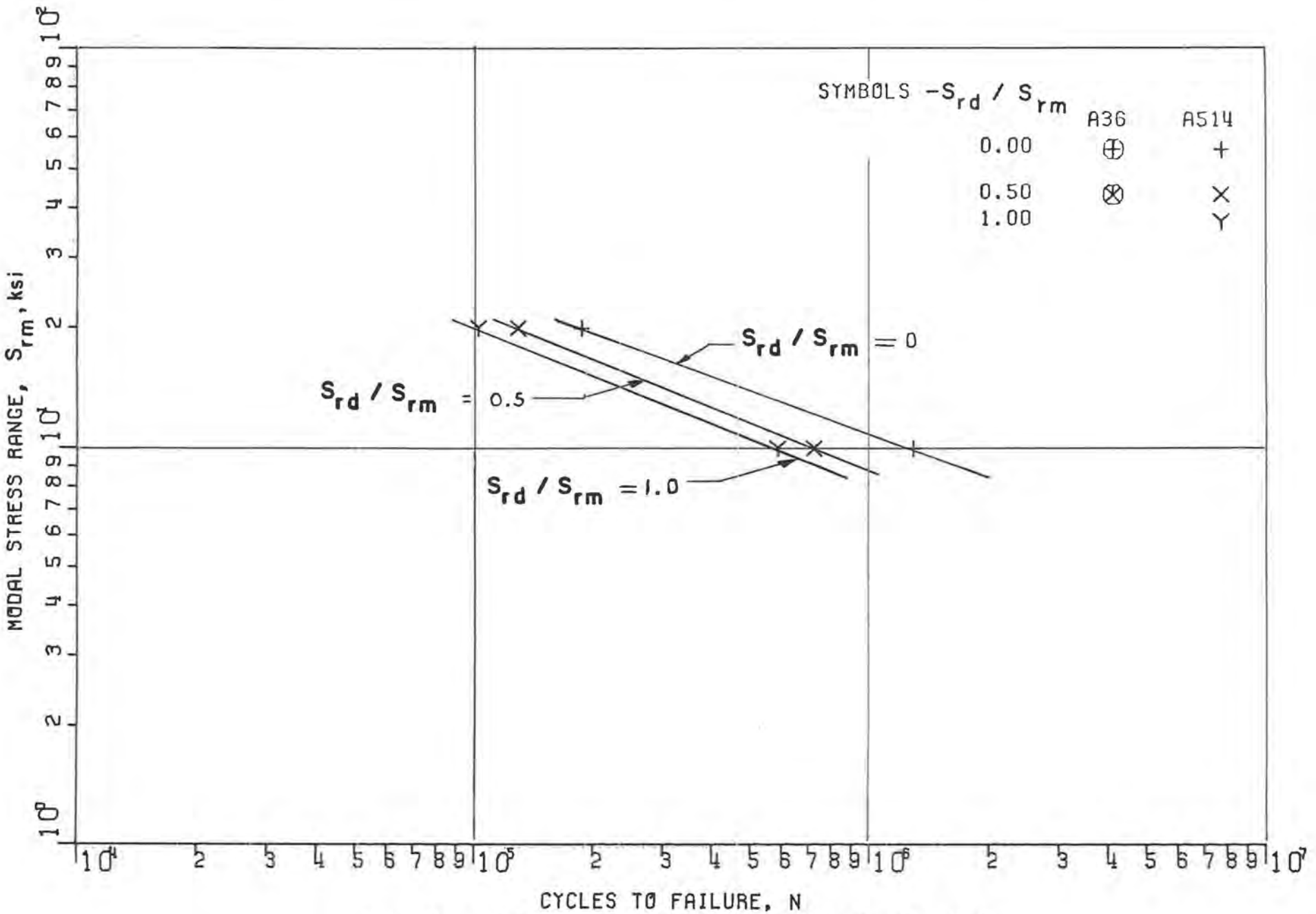

Figure 9. Modal stress range vs fatigue life for detail C.

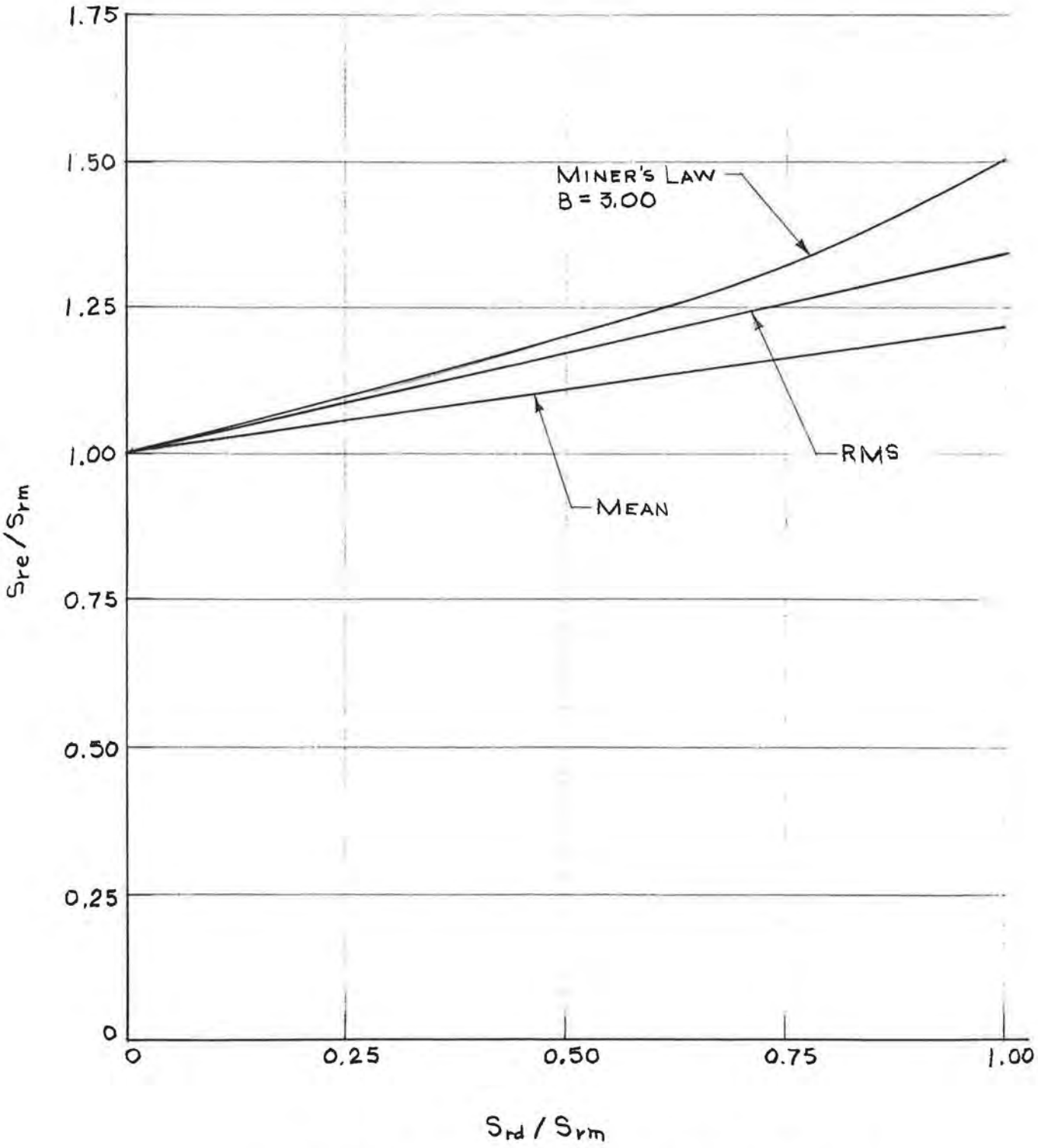

Figure 10. Variation in effective stress range.

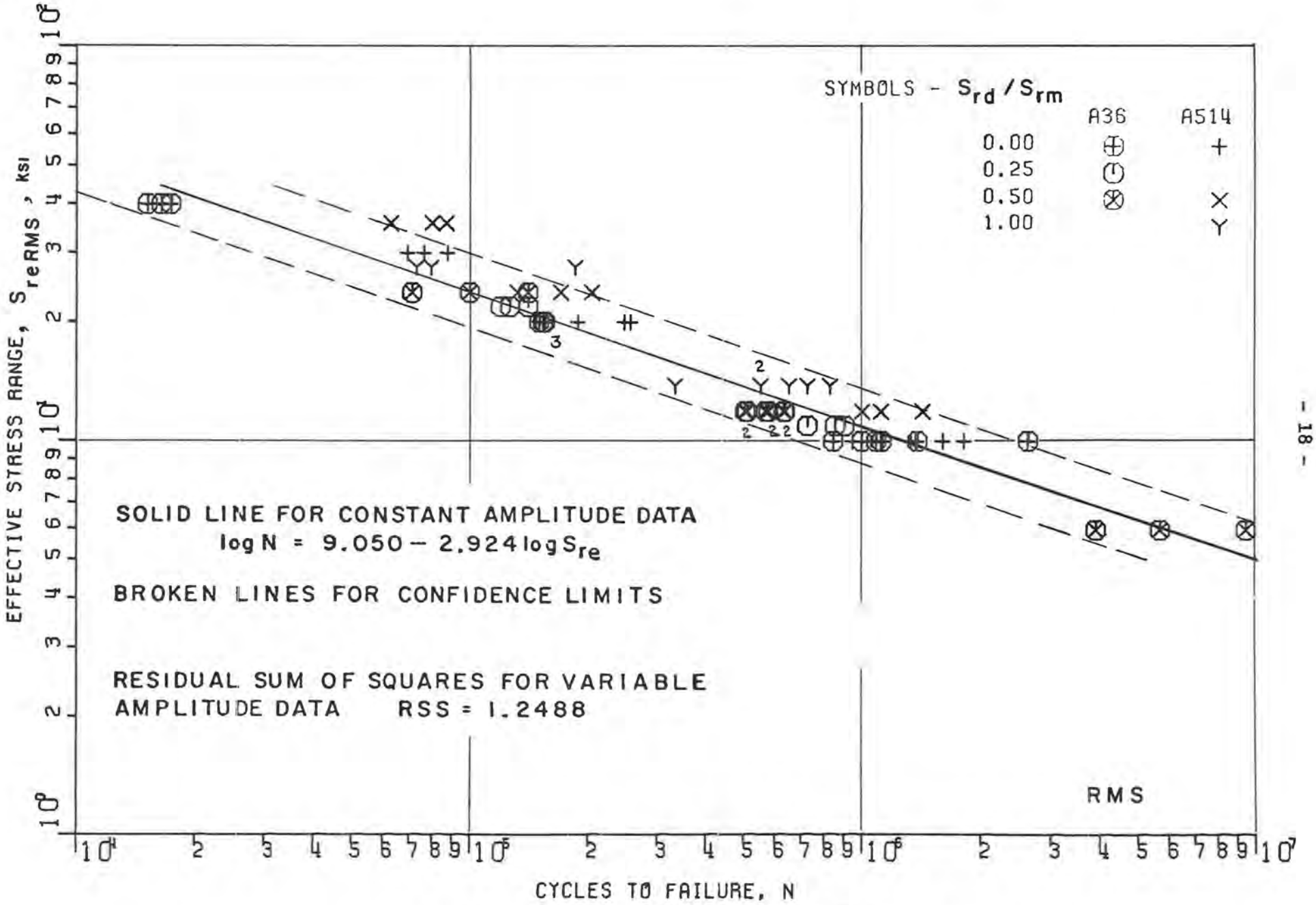

Figure 11. Data for detail C, in terms of $S_{re_{RMS}}$.

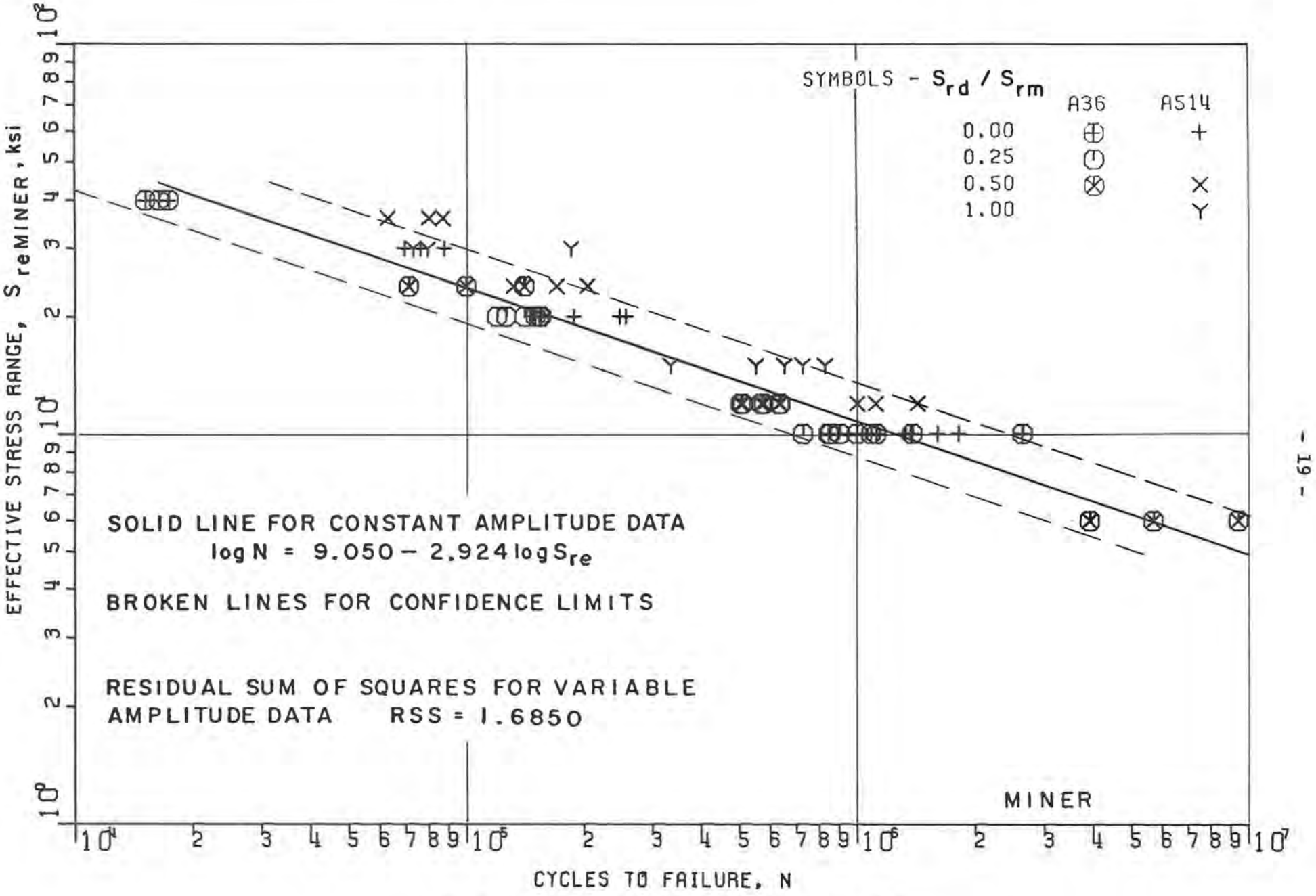

Figure 12. Data for detail C, in terms of S_{re} MINER.

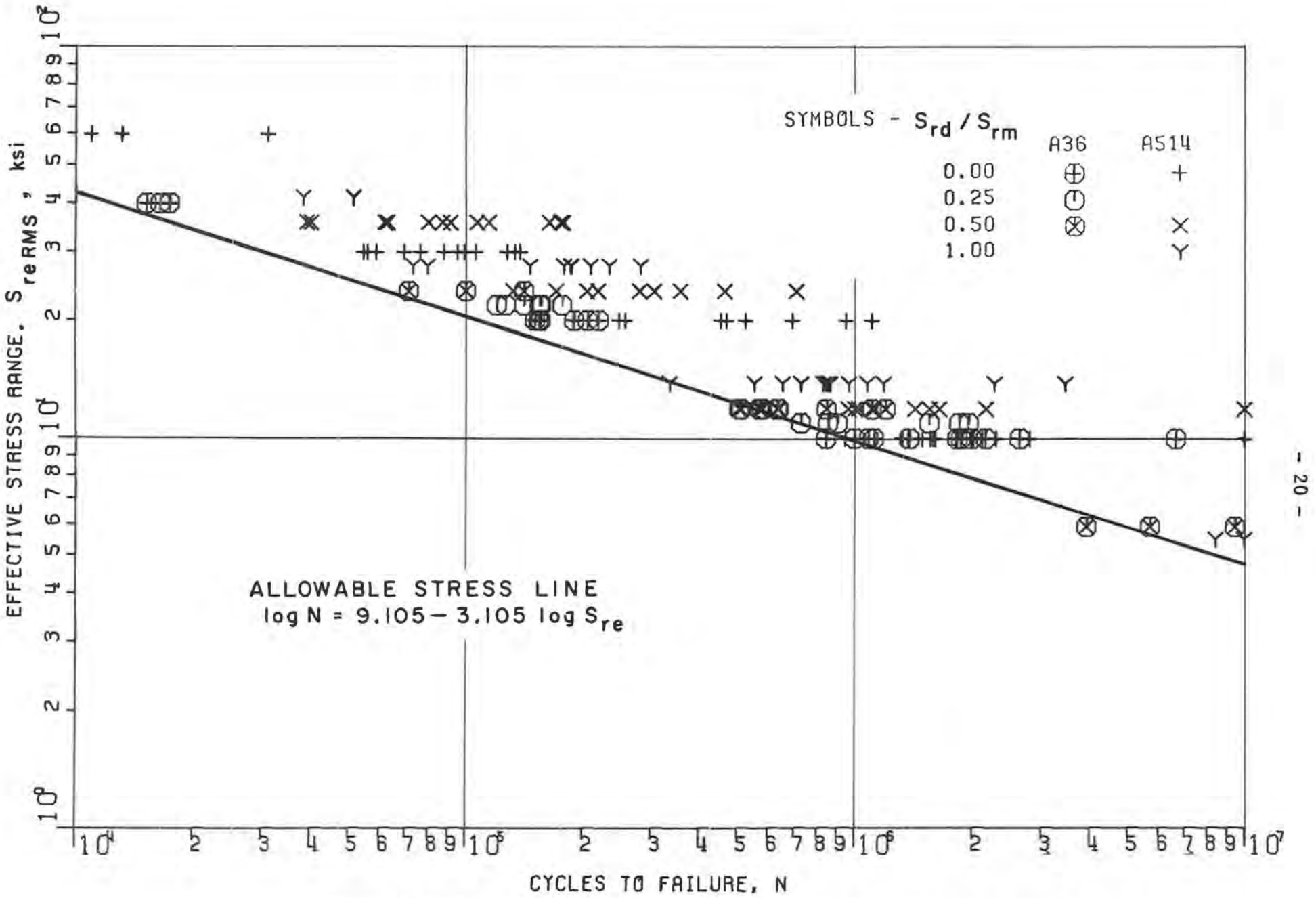

Figure 13. Comparison of cover-plated beam data from this study with AASHTO fatigue design provisions.

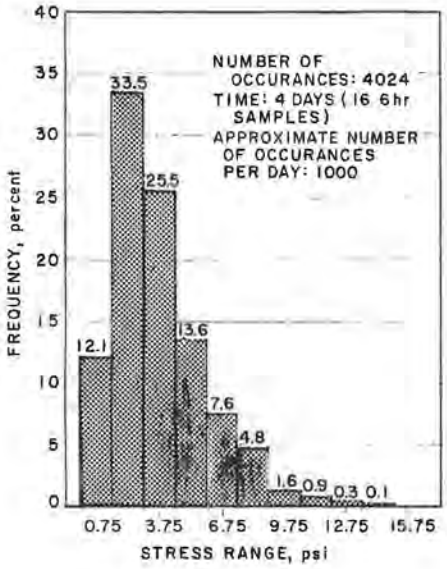

Histogram for
Hanger End Detail

Stress Spectrum, ksi

i	α_i	S_{ri}	$\alpha_i S^2_{ri}$
1	0.121	0.75	0.07
2	0.335	2.25	1.70
3	0.255	3.75	3.59
4	0.136	5.25	3.75
5	0.076	6.75	3.46
6	0.048	8.25	3.27
7	0.016	9.75	1.52
8	0.009	11.25	1.14
9	0.003	12.75	0.49
10	0.001	14.25	0.20
	1.000		19.19

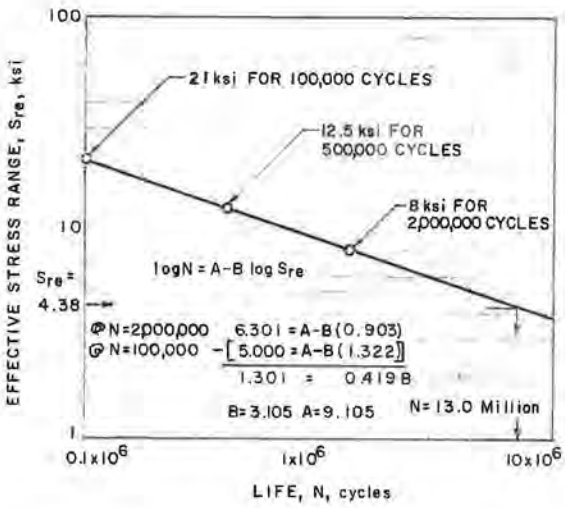

Allowable Effective Stress Range
for Hanger End Detail
(AASHTO Category E)

$$S_{re} = \sqrt{\sum \alpha_i S^2_{ri}} = \sqrt{19.19}$$

$$S_{re} = 4.38 \text{ ksi}$$

$$\log N = 9.105 - 3.105 \log (4.38)$$

$$N = 13 \times 10^6 \text{ cycles}$$

$$\text{Life in years } Y = \frac{13 \times 10^6}{1000 \times 365} = 35.6$$

Remaining life 35.6 - 10 = 25.6 years

Figure 14. Example of estimation of remaining life.